Folic acid radioconjugates: Müller and Schibli describe current folate receptor–targeting strategies and summarize the promise of several folic acid radioconjugates for SPECT and PET oncologic applications. . . . . ***Page 1***

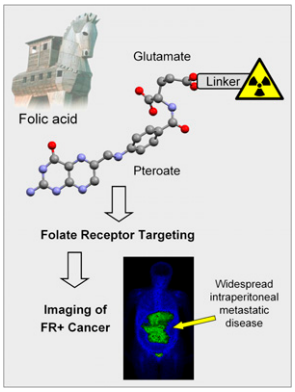

PET probe for melanoma: Minn and Vihinen offer commentary on current practices in PET staging of melanoma, focusing on a novel tracer described in this issue of *JNM* with potential for detection of regional lymph node metastases. . . . . ***Page 5***

Cortical networks and PET: Kumar and Chugani review the use of ^{18}F-FDG PET in elucidating cortical networks underlying a range of neurocognitive dysfunction and preview an article in this issue of *JNM* on its utility in postencephalitic epilepsy. . . . . ***Page 8***

Vascular inflammation and PET: Yoo and colleagues use ^{18}F-FDG PET to examine the severity of vascular inflammation in healthy individuals without hyperlipidemia but with elevated high-sensitivity C-reactive protein. . . . . ***Page 10***

Time corrections of tumor SUVs: Stahl and colleagues present a simple, algebraically deduced method using a single reference point to make straightforward time corrections of tumor SUVs in ^{18}F-FDG PET of breast cancer. . . . . ***Page 18***

^{11}C-PBR28 PET and translocator protein binding: Owen and colleagues explore whether mixed-affinity binding characteristics in multiple sclerosis can be detected in brain tissue and blood from individuals with no history of neurologic disease. . . . . ***Page 24***

^{11}C-PK11195 in vasculitides: Lamare and colleagues investigate whether PET/CT angiography using a selective ligand for the translocator protein 18 kDa, expressed in activated macrophages, can allow imaging and quantification of arterial wall inflammation in patients with large-vessel vasculitis. . . . . ***Page 33***

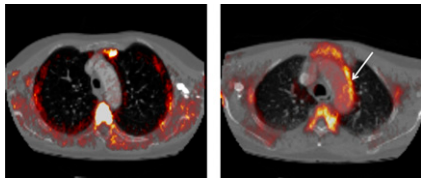

PET in FIRES: Mazzuca and colleagues describe the utility of ^{18}F-FDG PET in identifying the location of neocortical dysfunction in pediatric febrile infection–related epilepsy syndrome, a recently described entity of unknown etiology. . . . . ***Page 40***

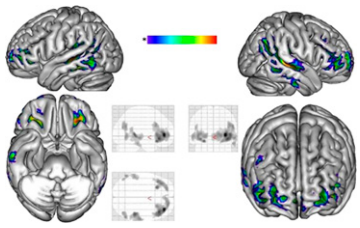

Monitoring antiangiogenic therapy response: de Langen and colleagues assess the predictive value of combined PET, CT, and MR data during antiangiogenic treatment in patients with advanced non–small cell lung cancer. . . . . ***Page 48***

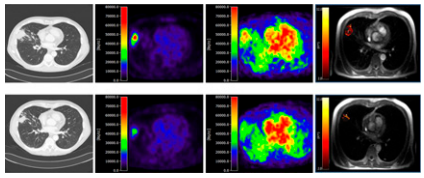

Follow-up scintigraphy in DTC: de Meer and colleagues question the value added by follow-up diagnostic radioiodine whole-body scintigraphy to recombinant human thyroid-stimulating hormone–stimulated thyroglobulin measurement in high-risk patients with differentiated thyroid cancer. . . . . ***Page 56***

Myocardial OEF and dynamic $^{15}O_2$ PET: Lubberink and colleagues determine the accuracy of oxygen extraction fraction measurements using a dynamic PET protocol after bolus inhalation of $^{15}O_2$. . . . . ***Page 60***

PET/CT after CRT: Uebleis and colleagues use electrocardiogram-gated ^{18}F-FDG PET/CT to identify differences in responders and nonresponders to cardiac resynchronization therapy, with results that could inform alternative and individualized therapies for nonresponders. . . . . ***Page 67***

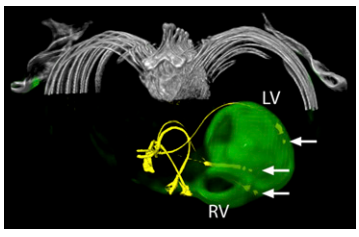

Localization with ^{90}Y PET/CT: Gates and colleagues evaluate the results of PET/CT imaging to determine ^{90}Y glass microsphere distribution in patients after implantation for transarterial radiation treatment of liver tumors. . . . . ***Page 72***

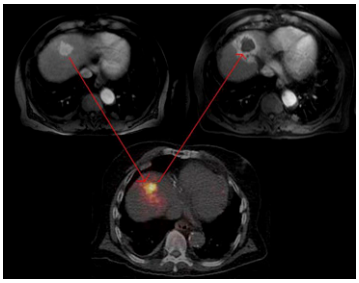

PET prediction in RA treatment: Elzinga and colleagues assess correlations between changes in ^{18}F-FDG joint uptake on PET after only 2 wk of infliximab treatment and later clinical outcomes in patients with rheumatoid arthritis. . . . . ***Page 77***

PET in prostate cancer: Jadvar provides an educational overview of the role of imaging in prostate cancer and the relative and respective capabilities of ^{18}F-FDG, ^{18}F- or ^{11}C-acetate, and ^{18}F- or ^{11}C-choline in PET imaging in the disease. . . . . ***Page 81***

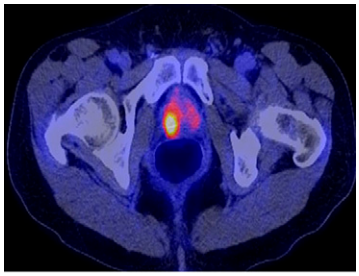

PET, ICH, and stem cells: Feng and colleagues use serial ^{18}F-FDG PET imaging to assess the efficacy of human mesenchymal stem cells in the treatment of intracerebral hematoma in a primate model.. . . . . ***Page 90***

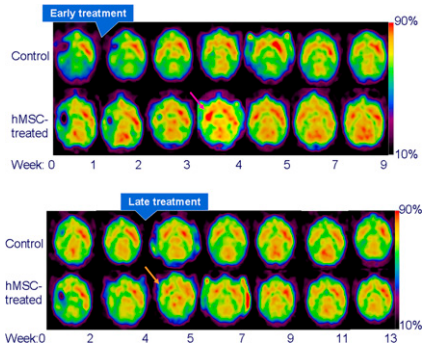

Choline metabolism in HCC: Kuang and colleagues examine the relationship between choline metabolism and tracer uptake in ^{11}C-choline PET imaging in an animal model of hepatocellular cancer. . . . . ***Page 98***

Imaging TSPO expression in glioma: Buck and colleagues describe preclinical PET studies characterizing a high-affinity aryloxyanilide-based translator protein imaging ligand, a candidate probe for quantitative assessment of translator protein expression in glioma. . . . . ***Page 107***

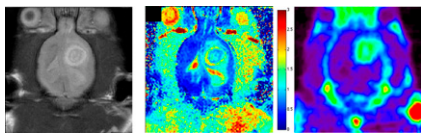

Melanoma lymphoscintigraphy with ^{18}F-MEL050: Denoyer and colleagues detail the efficacy of differing routes of administration of a new benzamide-based PET radiotracer for imaging regional lymph node metastasis in melanoma. . . . . ***Page 115***

^{68}Ga-DOTATOC reporter gene imaging: Zhang and colleagues report on a series of validation studies of the human somatostatin receptor subtype 2–^{68}Ga-DOTATOC reporter system and potential beneficial aspects in translation to clinical studies.. . . . . ***Page 123***

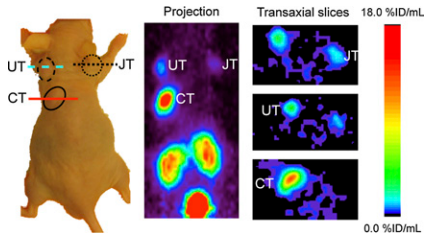

Comparing dopamine transporter tracers: Varrone and colleagues examine the kinetics and relative merits of ^{18}F-FE-PE2I, a novel radioligand for dopamine transporter PET, and ^{11}C-PE2I in nonhuman primates. . . . . ***Page 132***

PET and Abraxane treatment: Sun and colleagues investigate whether ^{18}F-FPPRGD2, an integrin-specific PET tracer, has utility in monitoring early response of breast tumors to Abraxane therapy in preclinical studies.. . . . . ***Page 140***

^{18}F-PFH PET for renal imaging: Awasthi and colleagues explore the potential of *p*-^{18}F-fluorohippurate for PET imaging to measure effective renal plasma flow and function. . . . . ***Page 147***

MRI-assisted PET motion correction: Catana and colleagues apply a novel algorithm for data processing and rigid-body motion correction for an MRI-compatible PET brain scanner prototype and describe the results of phantom and human validation studies. . . . . ***Page 154***

ON THE COVER

Head motion is difficult to avoid in long PET studies, degrading image quality and offsetting the benefit of using a high-resolution scanner. As a potential solution, simultaneously acquired MRI data can be used for motion tracking. The prototype dedicated brain scanner shown here, which can be operated inside the bore of an MRI scanner, has the potential to improve PET image quality and to benefit many neurologic applications.

See page 155.